Available online at BCREC website: https://bcrec.id

Bulletin of Chemical Reaction Engineering & Catalysis, 18 (1) 2023, 48-58

Research Article

Pillarization of Sumatera Bentonite by Sodium-assisted as Effective Adsorbent of Anionic Surfactants Sodium Lauryl Sulphate (SLS) Waste

Risfidian Mohadi[1,2,*], Yusuf Mathiinul Hakim[1], Rahma Dinta Astuti[2], Idha Royani[3], M. Mardiyanto[4]

[1]Graduate School, Faculty of Mathematics and Natural Sciences, Sriwijaya University, Palembang, 30139, South Sumatera, Indonesia.
[2]Department of Chemistry, Faculty of Mathematics and Natural Sciences, Sriwijaya University, Palembang, 30139, South Sumatera, Indonesia.
[3]Department of Physics, Faculty of Mathematics and Natural Sciences, Sriwijaya University, Palembang, 30139, South Sumatera, Indonesia.
[4]Pharmaceutical Department, Faculty of Mathematics and Natural Sciences, Sriwijaya University, Palembang, 30139, South Sumatera, Indonesia.

Received: 19th November 2022; Revised: 2nd February 2023; Accepted: 3rd February 2023
Available online: 6th February 2023; Published regularly: March 2023

Abstract

In this work, the Sumatera bentonite was sodium-pillarized in a new low-temperature and restricted time preparation route and then applied in anionic surfactant sodium lauryl sulphate removal. Structure characterization used Fourier Transform Infra Red (FT-IR), Scanning Electron Microscope - Energy Dispersive X-ray (SEM-EDX), X-ray Diffraction (XRD), and Brunauer–Emmett–Teller (BET) analysis. A strong peak at 22° and 35.66° in XRD analysis was detected as Sodium-pillar that increased crystallinity, then the functional changes of dehydration in lattice structure were detected in 1013 cm^{-1} by FTIR analysis. The morphology and compositional transformation were analyzed by SEM-EDX and BET analysis, denoted by increasing particle shape and sodium intercalant composition homogeneity. Moreover, the surface area increased from 61.791 to 66.086 m^2/g. The sodium lauryl sulphate adsorption by bentonite-Na reached maximum capacity at 8.403 mg/g, which is higher than the pristine bentonite (5.747 mg/g) under the optimum condition. The adsorption mechanism is feasible, endothermic, and conformed to the pseudo-second-order and Freundlich adsorption model. The new route proposed for sodium intercalation effectively improves the Sumatera bentonite adsorption ability to remove sodium lauryl sulphate waste.

Keywords: Low-temperature; Pillarization; Bentonite; Adsorption; Sodium Lauryl Sulphate

How to Cite: R. Mohadi, Y.M. Hakim, R.D. Astuti, I. Royani, M. Mardiyanto (2023). Pillarization of Sumatera Bentonite by Sodium-assisted As Effective Adsorbent of Anionic Surfactants Sodium Lauryl Sulphate (SLS) Waste. *Bulletin of Chemical Reaction Engineering & Catalysis*, 18(1), 48-58 (doi: 10.9767/bcrec.16500)

Permalink/DOI: https://doi.org/10.9767/bcrec.16500

1. Introduction

Surfactants are estimated to be used for 16.6 million tons in 2022 in personal care, household, cosmetics, foodstuffs, and agrochemicals to optimize the amphoteric property [1,2]. Surfactant waste is frequently disposed of straight into the environment. It triggers a hazardous effect on the human tissue system (like eye and skin irritation) and aquatic life for long-term accumulation [3]. Generally, anionic surfactants represent 60 % amount of surfactant pollution, contributed mainly by linear alkyl sulphonate (LAS) or sodium lauryl sulphate (SLS) [4].

* Corresponding Author.
Email: risfidian.mohadi@unsri.ac.id (R. Mohadi)

SLS is a synthetic anionic surfactant used in household products of soap, detergent, and other cleansing liquids. In a natural water system, 50% of surfactants are naturally degraded, 25% form a solid suspension, and then 25% is dissolved as a pollution compound; thus, its needs to be removed [5,6]. Conventional water treatment for surfactant waste included flocculation, coagulation, foam separation, Fenton oxidation, aerobic biodegradation, membrane filtration, and adsorption [7]. However, adsorption was chosen due to its economic and easy use, and considerable research has been reported to eliminate the most profitable and efficient adsorbent [8].

Bentonite was popularly utilized as a good precursor adsorbent due to its abundance and available multi-function features in modification [9]. The bentonite adsorption capability is driven by the exchangeable cations in the lattice structure of sandwiching layers, filled mainly by calcium, magnesium, and others [10,11]. Bentonite modification enlightens the adsorption capability via thermal activation, acid-base activation, pillarization/intercalation, ion exchange, and composite with other compounds [9]. Pillarization/intercalation is nominated as a simple method to increase the surface area of bentonite in the adsorption process. However, pillarization/intercalation needs high energy via thermal and long-time preparation [12,13]. According to literature observation, there is no updated report explaining the mechanism of low-temperature preparation in bentonite intercalation. Based on the Laipan report [14], an over-concentrated solution has a potential in the intercalation by intramolecular force of the particle into the interlayer structure.

In this work, the new route pillarization of Sumatera bentonite was proposed using saturated sodium under low-temperature and restricted time preparation then used as the SLS removal. Hopefully, this work provides a new perspective on SLS waste removal using a new route-prepared bentonite-based adsorbent. The bentonite-modified adsorbent was characterized by SEM-EDX, FT-IR, XRD, and BET analysis then the adsorption mechanism was studied by kinetic, thermodynamic, and isotherm adsorption models.

2. Materials and Methods

2.1 Chemicals and Instrumentations

The bentonite was imported from Sumatera, Indonesia (called Sumatera bentonite/SB). The pure-grade chemicals were purchased, such as sodium hydroxide (by Merck), chloride acid (by Merck), silver nitrate (by Sigma Aldrich), sodium chloride (by Merck), chloroform (by Sigma Aldrich), sodium lauryl sulphate ($C_{12}H_{25}OSO_3Na$/SLS by Sigma Aldrich), sodium dihydrogen phosphate monohydrate (by Sigma Aldrich), 0,5% phenolphthalein indicator solution (by Merck), and methylene blue (by Sigma Aldrich). The characterization of adsorbent was conducted by using JSM 6510-LA SEM-EDX with 20 kV energy scanning and 10,000 magnifications, Rigaku Mini-flex600 XRD was used scanning speed 1 deg/min from 2θ range 10-90°, Perkin-Elmer UATR Spectrum two FT-IR instrumentation within range of 400-4000 cm^{-1}, and Surface Area Analyzer of Quantachrome ASIQ-win v.3.01 based on BET calculation. The reducing concentration of SLS was analyzed by spectrophotometer UV-Vis Bio-Base BK-UV 1800 PC at 652 nm (methylene blue standard wavelength).

2.2 Bentonite Pillarization

The pristine bentonite modification was approached by saturated sodium chloride solution intercalation (with the composition of bentonite 100 g and sodium chloride 333 mL) under room temperature for 120 min, followed by distilled water dissolution for 10 minutes (the ratio of the mixture to distilled water is 1:2). The precipitate was separated and washed with heated distilled water. Re-dissolved in 333 mL saturated sodium chloride solution for 120 min, mixing under room temperature. The filtrate solution was checked for Cl^- excess by adding the silver nitrate as an indicator. The clear precipitate was calcined at a temperature of 200 °C for 12 h. This material is denoted as bentonite-Na (B-Na).

2.3 Adsorption Work

The adsorption work was initiated by varying the doses in the 0.01, 0.02, 0.03, 0.04, 0.05, and 0.06 g. Next, the effect of adsorption time was analyzed by variation time 0, 10, 20, 30, 40, 50, and 60 min in the adsorbent composition of 0.02 g/50 mL SLS sample. The adsorption mechanism was studied by varying temperatures 30, 40, 50, 60, and 70°C, then varying concentrations of SLS sample 2, 4, 6, 8, and 10 mg/L in composition adsorbent 0.04 g/50 mL sample for 30 min. The excess filtrate concentration was measured by the MBAS (Methylene Blue Active Substances) method [15,16].

The MBAS method was detailed by following steps: the filtrate was separated and added

by solutions of phenolphthalein 3-5 drops and 1 N of NaOH drop by drop until the solution color changed to pink and added by H_2SO_4 drop by drop to remove the color. Then, the solution was added by 3.125 mL methylene blue solution and 2.5 mL chloroform solution. The solution was shaken for 30 s and aged for phase separation. The separate phase of chloroform was drawn off into the second funnel, then repeat the extraction of solution in the first funnel was repeated twice with 10 mL chloroform each time. The 6.25 mL of wash solution was added to the second funnel, shaken for 30 s, and aged for phase separation. Next, the washed chloroform layer was drawn off, and the spectrophotometer UV-Vis measured the absorbances of sample solutions at a maximum wavelength of 652 nm (with a blank of chloroform).

Preparation of methylene blue and washing solution was adapted by following steps: methylene blue solution was composed of mixing of 30 mL of methylene blue 1000 mg/L, 41 mL of H_2SO_4 6 N, 50 g of NaH_2PO_4, and distilled water in 1000 mL dilution flask. Next, the washing solution was prepared by mixing 41 g of H_2SO_4 6N, 50 g of $Na_2H_2PO_4$, and distilled water in a dilution flask of 1000 mL.

2.4 Analysis of Adsorption Mechanism

According to the literature, the determination of adsorption kinetics of pseudo-first-order and pseudo-second-order models are figured out in Equations (1) and (2), respectively [17]:

$$\ln\left(q_e - q_t\right) = \ln q_e - tK_1 \tag{1}$$

$$\frac{t}{q_t} = \frac{1}{q_e^2 K_2} + \frac{t}{q_e} \tag{2}$$

where, q_e and q_t are defined as adsorption capacity at equilibrium and definite time, respectively, then K_1 and K_2 are the rate adsorption of pseudo-first-order (min^{-1}) and pseudo-second order ($g.mg^{-1}.min^{-1}$), respectively, then the t for time (min).

The effect of thermodynamic changes considered by the formula [18]:

$$\Delta G° = -RT \ln K_d \tag{3}$$

$$\Delta G° = \Delta H° - T\Delta S° \tag{4}$$

$$\ln K_d = \frac{\Delta S°}{R} - \frac{\Delta H°}{RT} \tag{5}$$

where, $\Delta G°$, $\Delta H°$, and $\Delta S°$ described as the value of Gibbs energy (kJ/mol), enthalpy changes (kJ/mol), and entropy changes (kJ/mol.K), respectively, then R is the standard gas constant

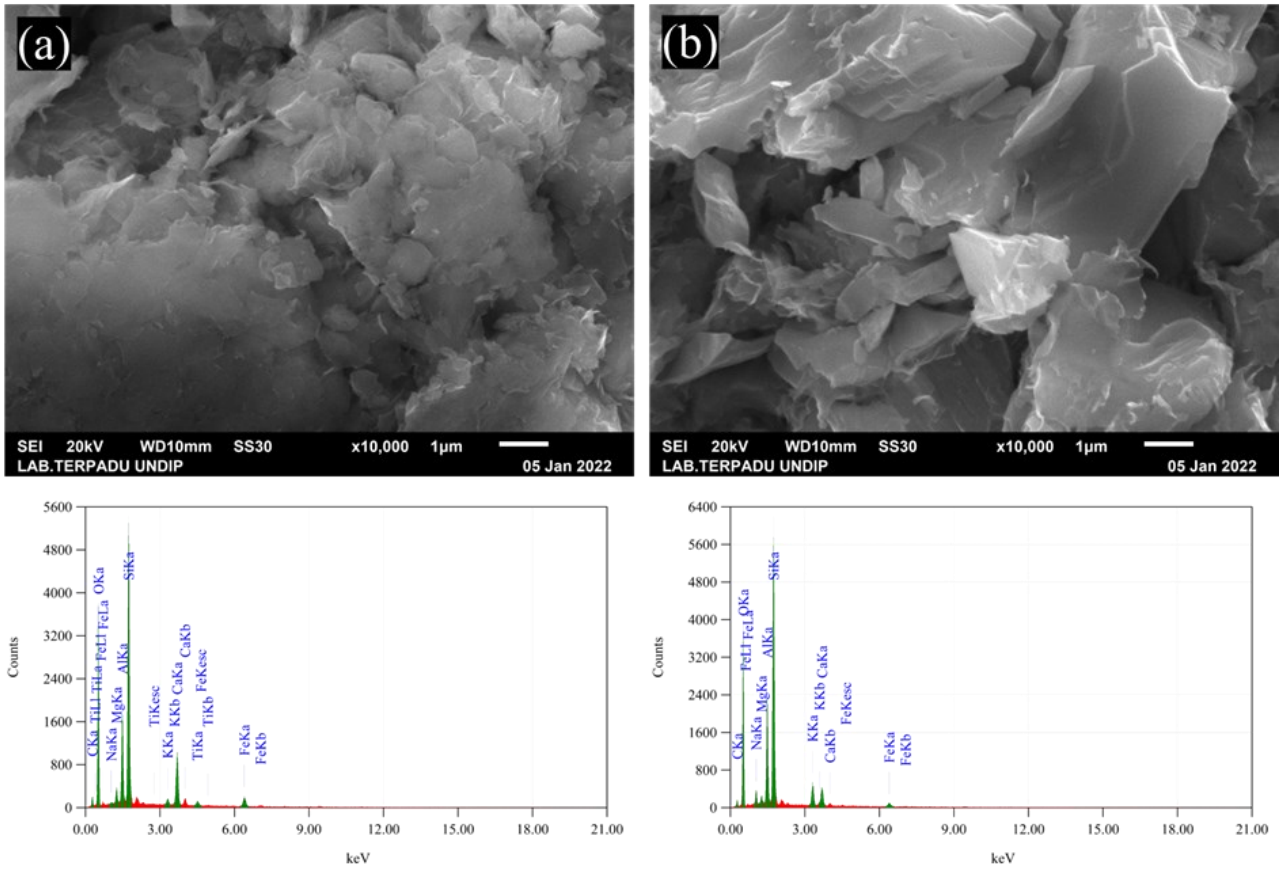

Figure 1. SEM visualization of Sumatera Bentonite (SB) (a) and Bentonite-Na (B-Na) (b).

(8.324 kJ/mol), T is temperature reaction (K), and K_d is the equilibrium constant.

Furthermore, the isotherm adsorption was considered by Langmuir and Freundlich isotherm model and measured by Equations (6) and (7) [19]:

$$\frac{C_e}{q_e} = \frac{1}{q_{\max} K_L} + \frac{C_e}{q_{\max}} \quad (6)$$

$$\ln q_e = \ln K_F + \frac{\ln C_e}{n} \quad (7)$$

where, q_e and q_{max} are denoted as capacity adsorption at equilibrium and maximum phase, respectively (mg/g), C_e is final concentration equilibrium (mg/L), K_L is constant of Langmuir adsorption (L/mg), then K_f and n are constant of Freundlich adsorption (L/g).

3. Results and Discussion

This work proposed a new route of bentonite sodium intercalation under low-temperature and restricted time preparation to produce an adsorbent to SLS waste. Removal of SLS waste is demanding due to the high volume of waste disposed of, triggering several disadvantages: life health, water quality, and increasing undesirable foam [20,21]. The economic discovery of adsorbent material applied in SLS waste treatment was established as a bright solution [22]. Here, we report the result of bentonite modification as an adsorbent agent of SLS waste.

The morphology and composition of materials according to SEM-EDX analysis are shown in Figure 1 and Table 1. The pillarization has expanded the layered structure of B-Na due to intramolecular force from intercalant that increases the swelling capacity [23]. According to the EDX data, intercalation affects lattice and interlayer structure. The evidence showed by increasing Na^+ composition in B-Na, while decreasing Fe^+, Mg^+, and Ca^+ as cation interlayers in SB. Conversely, crystallinity increase was recorded as additional Si^+ and Al^+ compositional in B-Na. The absence of the Ti^+ compound from B-Na means this phase has no impurities [24].

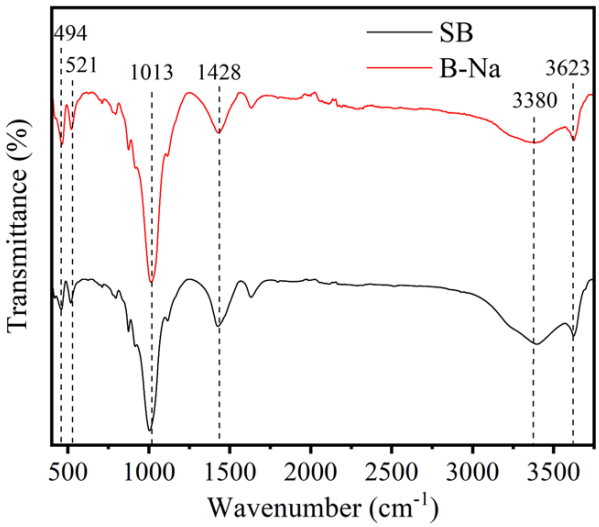

Figure 2. FTIR spectra of Sumatera Bentonite (SB) and Bentonite-Na (B-Na).

FTIR analysis shows the functional group transformation using wavelength movement displayed in Figure 2. The slight movement in the most substantial spectra of B-Na in 1013 cm^{-1} is dedicated to Si–O stretching vibration inside the tetrahedral framework of the montmorillonite layer [25]. The movement and decreasing intensity in the band 1428 cm^{-1} and 3380 cm^{-1} are related to H–O–H bending and stretching of the tetrahedra framework. The decreasing intensity was also observed in the band 2623 cm^{-1}, confirming the transformation of OH stretching from the montmorillonite framework [26]. Different bands of fingerprint region were recorded in 494 and 521 cm^{-1} for indication vibration band of Si–O–Si and Si–O–Al, respectively [27].

Fundamentally, there is no significant change in B-Na from the pure one, SB. However, the reduction intensity of the OH group was detected due to intercalation and calcination [27,28]. The slight intensity reduction at 845 cm^{-1} is associated with the decomposition of quartz crystals in B-Na [29].

The XRD pattern of B-Na and SB is displayed in Figure 3. According to the JCPDS file numb. 46-1045, the XRD pattern of bentonite can be analyzed as quartz mineral that emerged at 26.8°. The intensity of a quartz mineral at 26.8° was reduced due to structural transformation after pillarization and ampli-

Table 1. EDX composition of Bentonite-based adsorbent.

Compound	Sumatera Bentonite (mass%)	Bentonite-Na (mass%)
C	10.74	9.63
O	56.23	55.26
Na	0.13	1.65
Mg	1.07	0.57
Al	5.47	7.40
Si	17.37	19.66
K	0.55	2.45
Ca	5.08	2.13
Ti	0.64	-
Fe	2.72	1.25

fied by increasing peak intensity at 22° and 35.66° associated with montmorillonite mineral formation [30]. The high crystallinity of montmorillonite confirmed the FTIR analysis [28,31].

The textural characteristics of SB and B-Na were analyzed by adsorption-desorption of nitrogen at 77.35 K. Figure 4 displayed the isotherm characteristics of nitrogen adsorption-desorption of nitrogen by SB and B-Na. The graphical plot shows that both SB and B-Na followed type IV isotherm according to Brunnauer-Deming-Teller (BDT) classification [32]. Overlapping of adsorption-desorption point data plotting started from the low relative pressure around 0.45 and showed a hysteresis type H3. This characteristic includes material in mesopore layered material [33].

BET model was used in specific surface area parameter calculation of SB and B-Na as tabulated in Table 2. According to Table 2, the surface area of SB was lower than the B-Na. Finally, it confirmed that the improving interlayer of B-Na is due to the intercalation process that triggers the increasing active surface area for the adsorption mechanism. The pore diameter and pore volume calculated based on Barrett-Joyner-Halenda (BJH) method show decreasing value due to increased crystallinity that changes the structural compositional and pore surfaces [33]. However, the interlayer lifting provides a wider active surface area.

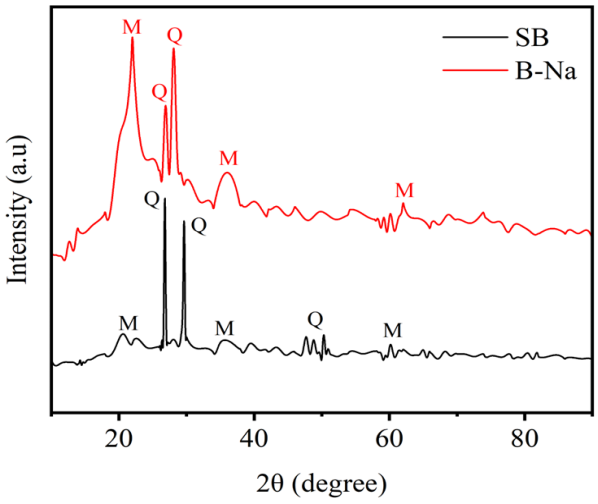

Figure 3. XRD pattern of adsorbent (Sumatera Bentonite (SB); Bentonite-Na (B-Na)).

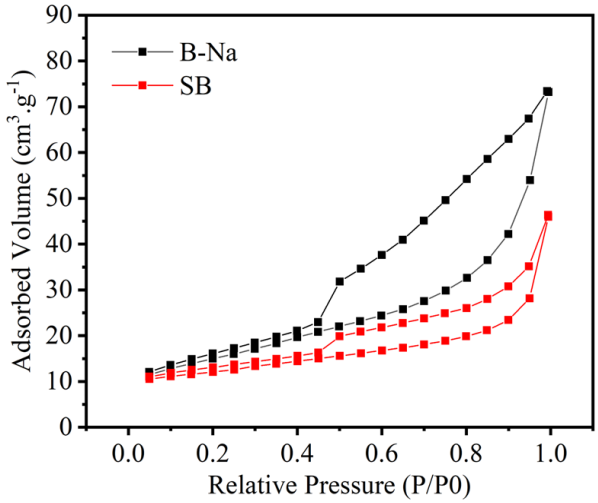

Figure 4. N_2 adsorption-desorption characteristics of Bentonite-based adsorbent.

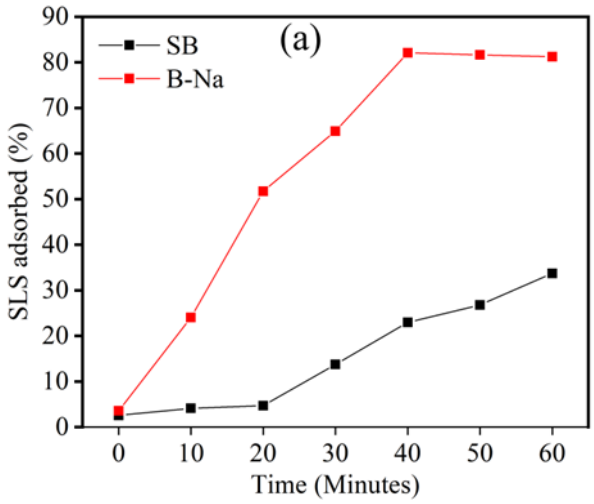

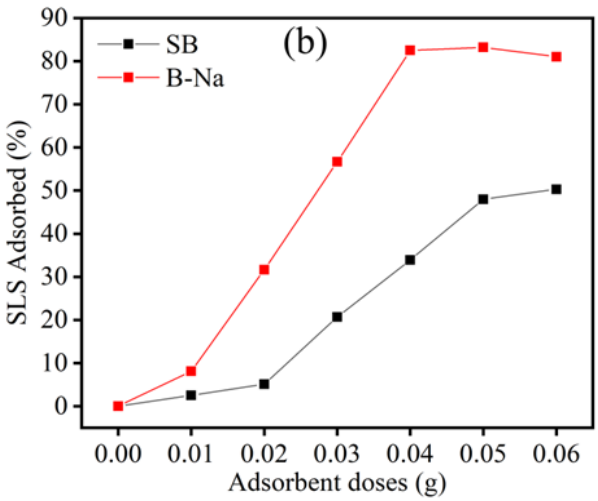

Figure 5. Effect of adsorption time (a) and adsorbent doses (b) of Bentonite-based adsorbent.

Table 2. The BET surface area analysis, pore diameter, and pore volume of Bentonite-based adsorbent.

Adsorbent	BET Surface Area (m^2/g)	Pore Diameter (nm)	Pore Volume (cm^3/g)
Sumatera Bentonite	61.791	4.678	0.144
Bentonite-Na	66.086	4.279	0.141

The characterization materials show integration information of adsorption synergism in the bentonite-modified adsorbent. The expanded materials shown in SEM analysis support the higher crystallinity condition affected by the intercalation process according to XRD analysis [34]. Moreover, the functional group transformation detected in FTIR analysis and BET surface area analysis supports the proposed adsorption mechanism dominated by direct interaction between adsorbent and adsorbate [35].

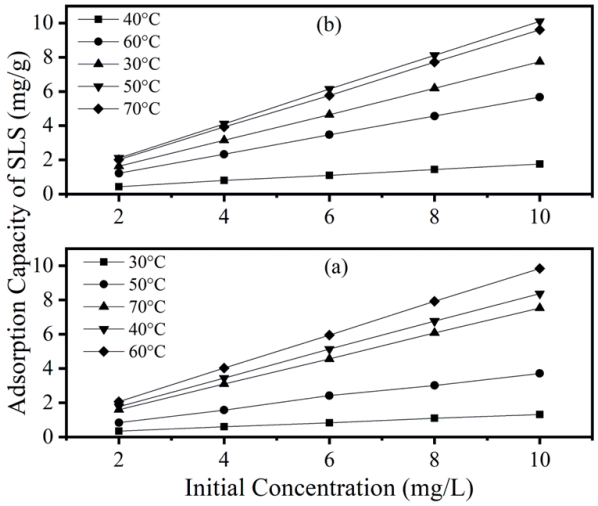

Figure 6. The Effect of Temperature and Initial Concentration Adsorption of SLS Waste Using Sumatera Bentonite (SB) (a) and Bentonite-Na (B-Na) (b).

The SLS wastewater adsorption was studied using the modified and pure bentonite according to the kinetics, isotherm, and thermodynamics model. Figure 5 showed the SLS adsorption using B-Na pillarized reached the equilibrium for 40 min of adsorption time. A prior report described the impact of intercalation increasing the active site from the pure bentonite; thus, increasing the active site triggers a high rate of adsorption [14]. Figure 5(b) shows the most effective adsorbent doses were used at doses 0.04 g adsorbent.

The kinetic adsorption was calculated by adopting pseudo-first-order (PFO) and pseudo-second-order (PSO) models [36]. Table 3 shows

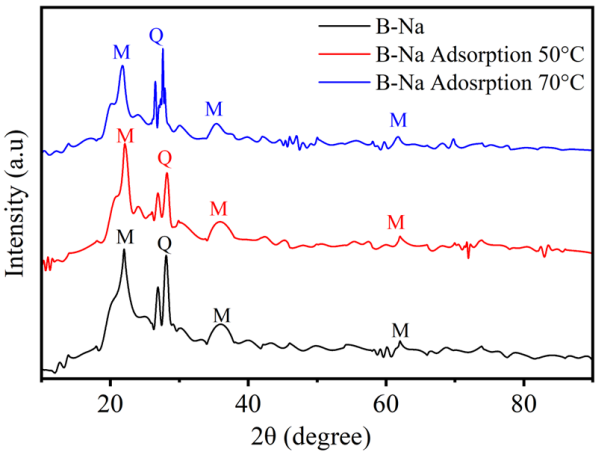

Figure 7. XRD pattern of Bentonite-based adsorbent on different temperature adsorption.

Table 3. Kinetics adsorption of SLS waste using Sumatera Bentonite (SB) and Bentonite-Na (B-Na).

Adsorbent	C_0 (mg/L)	q_e (mg/L)	PFO			PSO		
			$q_{e\ calc}$ (mg/g)	R^2	K_1 (min^{-1})	$q_{e\ calc}$ (mg/g)	R^2	K_2 (min^{-1})
Sumatera Bentonite	1.054	0.843	1.008	0.8078	0.031	0.855	0.925	0.062
Bentonite-Na		1.62	4.345	0.059	0.049	1.704	0.8758	0.092

Table 4. Isotherm adsorption of SLS waste using Sumatera Bentonite (SB) and Bentonite-Na (B-Na).

Adsorbent	Temperature (K)	Langmuir model isotherm			Freundlich model isotherm		
		q_{max} (mg/g)	K_L	R_1	n	K_F	R_2
Sumatera Bentonite	303	1.234	3.958	0.807	1.217	4.66	0.999
	313	1.149	3.184	0.896	1.195	3.44	0.999
	323	5.747	0.270	0.829	1.114	1.54	0.996
	333	5.708	0.242	0.826	1.101	1.38	0.999
	343	5.102	0.247	0.829	1.1	1.26	0.999
Bentonite-Na	303	6.287	0.046	0.807	1.061	0.94	0.999
	313	6.377	0.083	0.887	1.095	1.72	0.999
	323	8.403	0.044	0.895	1.066	2.57	0.999
	333	8.237	0.047	0.895	1.110	2.45	0.999
	343	7.230	0.058	0.895	1.094	2.26	0.998

Table 5. Thermodynamic parameter adsorption of SLS waste using Sumatera Bentonite (SB) and Bentonite-Na (B-Na).

Concentration	Adsorbent	T (K)	q_e (mg/g)	ΔH (kJ/mol)	ΔS (kJ/mol)	ΔG (kJ/mol)
2 mg/L	SB	303	0.34	52.256	0.166	2.065
		313	0.44			0.408
		323	0.83			−1.248
		333	1.22			−2.905
		343	1.59			−4.561
	B-Na	303	1.63	19.88	0.074	−2.481
		313	1.77			−3.219
		323	2.11			−3.957
		333	2.06			−4.695
		343	2.02			−5.433
4 mg/L	SB	303	0.60	55.778	0.168	4.843
		313	0.81			3.162
		323	1.56			1.481
		333	2.33			−0.200
		343	3.10			−1.881
	B-Na	303	3.15	18.997	0.07	−2.223
		313	3.44			−2.923
		323	4.11			−3.624
		333	4.02			−4.324
		343	3.92			−5.024
6 mg/L	SB	303	0.82	57.513	0.173	5.067
		313	1.11			3.336
		323	2.42			1.605
		333	3.47			−0.126
		343	4.55			−1.857
	B-Na	303	4.65	17.692	0.066	−2.175
		313	5.13			−2.830
		323	6.14			−3.486
		333	5.95			−4.142
		343	5.76			−4.797
8 mg/L	SB	303	1.08	57.722	0.173	5.156
		313	1.45			3.421
		323	3.01			1.686
		333	4.56			−0.049
		343	6.08			−1.784
	B-Na	303	6.18	18.22	0.067	−2.101
		313	6.76			−2.771
		323	8.11			−3.442
		333	7.92			−4.112
		343	7.71			−4.783
10 mg/L	SB	303	1.31	58.363	0.175	5.255
		313	1.77			3.502
		323	3.67			1.749
		333	5.67			−0.003
		343	7.58			−1.756
	B-Na	303	7.73	17.878	0.066	−2.069
		313	8.36			−2.727
		323	10.09			−3.385
		333	9.84			−4.044
		343	9.59			−4.702

that the SLS adsorption conforms with the PSO kinetics model due to R^2 being closer to the value of 1. The PSO kinetics model explains that the adsorption mechanism is chemisorption, which means chemical bonding should occur [37].

According to Figure 6, the SLS adsorbed is affected by the increasing temperature adsorption. The optimum temperature adsorption using SB is 60 °C, while B-Na is 50 °C. It is evidenced that B-Na utilization as an adsorbent is more effective and low-cost due to lower temperature. The data of various temperature and concentration adsorption then be analyzed to determine the parameter of isotherm adsorption using the Langmuir and Freundlich isotherm model [38]. Different temperature adsorption (50 and 70 °C) was checked as additional information about the effect of adsorption temperature in structural transformation, and it concluded that temperature adsorption did not affect crystallinity changes. This statement is evidenced by XRD analysis in Figure 7.

The Langmuir model was developed to explaining solid-gas adsorption, then updated for different adsorbents [39]. This scheme assumes that the adsorption occurs by monolayer adsorption, thus no specific interactions between adsorbate molecules [40]. Additionally, the Freundlich model figured that adsorption occurred by multilayer in heterogeneous places [41]. Table 4 shows that Freundlich isotherm is appropriate in SLS adsorption using SB and B-Na associated with an R^2 value closer to 1. The adsorption capacity (Q_m) displayed Q_m of SLS using B-Na of 8.403 mg/g, while the Q_m of SLS using SB of 5.747 mg/g.

The thermodynamic parameters produce the data of ΔG, ΔH, and ΔS according to the literature [42] and are shown in Table 5. The ΔH analysis shows that the adsorption occurs endothermically due to the positive value of the ΔH. The mechanism can be predicted by ΔH value with an assumption that interactions of SLS adsorbate and adsorbent via hydrophilic, π-cationic, and electrostatic bonding endothermically [43]. The hydrophilic interaction supported by electrostatic bonding of surfactant active site towards electrophilic area in interlayer bentonite. Specifically, chemisorption occurs in SB adsorption due to ΔH more than 40 kJ/mol, while physisorption occurs in B-Na adsorption due to ΔH 0-40 kJ/mol [44,45]. Additionally, the negative value of ΔG describes that the adsorption is feasible and spontaneously occurs in nature; thus, the process requires high-temperature adsorption. Furthermore, the positive value of ΔS described the increasing irregularity interaction between adsorbate particles in the form of liquid to solid adsorbent [46].

Table 6 compares several adsorbents and their application to the anionic surfactant. According to the latest work, here is new data on bentonite-based adsorbent applied in SLS waste removal.

4. Conclusions

In conclusion, the new route of sodium intercalation in Sumatera bentonite was successfully proposed under low-temperature and restricted time preparation, then applied in SLS waste removal by adsorption. Several methods of material characterization declared the suc-

Table 6. Comparison adsorption ability of several adsorbent to anionic surfactant.

Adsorbent	Anionic surfactant	Adsorption Capacity (mg/g)	References
Lula soil sediment	Sodium dodecylbenzene sulfonate	0.865	[47]
Dickinson bayou soil sediment	Sodium dodecylbenzene sulfonate	9.674	
	Sodium hexadecyl diphenyl oxide disulfonate	4.963	
Silica	Sodium dodecyl sulphate	0.2	[48]
Ca-montmorillonite	Alkyl ethoxy carboxylate	0.23	[49]
Kaolinite		0.17	
Quartz/clay	Sulfosuccinate sodium salt (Aerosol-OT)	0.046	[50]
Sumatera bentonite	Sodium Lauryl Sulphate	5.747	This study
Bentonite-Na		8.403	

cessful modification. A study of the SLS removal using bentonite-based adsorbent reached the optimum condition for 40 minutes of adsorption and 0.04 g adsorbent used for adsorption capacity of bentonite-Na at 8.403 mg/g, higher than the Sumatera bentonite (5.747 mg/g). The adsorption dominate occurs by physisorption and is spontaneously endothermic.

Acknowledgment

The authors acknowledge support by the Inorganic and Environmental Chemistry and all members of Dr.rer.nat. Risfidian Mohadi research group at the Faculty of Mathematics and Natural Sciences, Sriwijaya University.

References

[1] Smithers team (2017). The Future of Surfactants to 2022. In: Smithers. https://www.smithers.com/services/market-reports/materials/the-future-of-surfactants-to-2022. Accessed 4 Nov 2022.

[2] Aslam, R., Mobin, M., Aslam, J., Aslam, A., Zehra, S., Masroor, S. (2021). Application of surfactants as anticorrosive materials: A comprehensive review. *Advances in Colloid and Interface Science*, 295, 102481. DOI: 10.1016/j.cis.2021.102481.

[3] Asio, J.R.G., Garcia, J.S., Antonatos, C., Sevilla-Nastor, J.B., Trinidad, L.C. (2023). Sodium lauryl sulfate and its potential impacts on organisms and the environment: A thematic analysis. *Emerging Contaminants*, 9(1), 100205. DOI: 10.1016/j.emcon.2023.100205.

[4] Karray, F., Mezghani, M., Mhiri, N., Djelassi, B., Sayadi, S. (2016). Scale-down studies of membrane bioreactor degrading anionic surfactants wastewater: Isolation of new anionic-surfactant degrading bacteria. *International Biodeterioration & Biodegradation*, 114, 14–23. DOI: 10.1016/j.ibiod.2016.05.020.

[5] Yüksel, E., Şengil, İ.A., Özacar, M. (2009). The removal of sodium dodecyl sulfate in synthetic wastewater by peroxi-electrocoagulation method. *Chemical Engineering Journal*, 152(2–3), 347–353. DOI: 10.1016/j.cej.2009.04.058.

[6] Azizullah, A., Khan, S., Rehman, S., Taimur, N., Häder, D.-P. (2021). Detergents Pollution in Freshwater Ecosystems. In: *Anthropogenic Pollution of Aquatic Ecosystems*. Cham: Springer International Publishing, pp. 245–270. DOI: 10.1007/978-3-030-75602-4_12.

[7] Mohammad, A., Ahmad, K., Rajak, R., Mobin, S.M. (2019). Remediation of Water Contaminants. In: *Handbook of Ecomaterials*. Cham: Springer International Publishing, pp. 373–391. DOI: 10.1007/978-3-319-68255-6_147.

[8] Momina, M., Ahmad, K. (2023). Feasibility of the adsorption as a process for its large scale adoption across industries for the treatment of wastewater: Research gaps and economic assessment. *Journal of Cleaner Production*, 388, 136014. DOI: 10.1016/j.jclepro.2023.136014.

[9] Borah, D., Nath, H., Saikia, H. (2022). Modification of bentonite clay & its applications: a review. *Reviews in Inorganic Chemistry*, 42(3), 265–282. DOI: 10.1515/revic-2021-0030.

[10] Ma, J., Qi, J., Yao, C., Cui, B., Zhang, T., Li, D. (2012). A novel bentonite-based adsorbent for anionic pollutant removal from water. *Chemical Engineering Journal*, 200–202, 97–103. DOI: 10.1016/j.cej.2012.06.014.

[11] Cherian, C., Arnepalli, D.N. (2015). A Critical Appraisal of the Role of Clay Mineralogy in Lime Stabilization. *International Journal of Geosynthetics and Ground Engineering*, 1(1), 8. DOI: 10.1007/s40891-015-0009-3.

[12] Shattar, S.F.A., Zakaria, N.A., Foo, K.Y. (2017). Utilization of montmorillonite as a refining solution for the treatment of ametryn, a second generation of pesticide. *Journal of Environmental Chemical Engineering*, 5(4), 3235–3242. DOI: 10.1016/j.jece.2017.06.031.

[13] Kaufhold, S., Dohrmann, R. (2009). Stability of bentonites in salt solutions | sodium chloride. *Applied Clay Science*, 45(3), 171–177. DOI: 10.1016/j.clay.2009.04.011.

[14] Laipan, M., Xiang, L., Yu, J., Martin, B.R., Zhu, R., Zhu, J., He, H., Clearfield, A., Sun, L. (2020). Layered intercalation compounds: Mechanisms, new methodologies, and advanced applications. *Progress in Materials Science*, 109, 1–97. DOI: 10.1016/j.pmatsci.2019.100631.

[15] Wyrwas, B., Zgoła-Grześkowiak, A. (2014). Continuous Flow Methylene Blue Active Substances Method for the Determination of Anionic Surfactants in River Water and Biodegradation Test Samples. *Journal of Surfactants and Detergents*, 17(1), 191–198. DOI: 10.1007/s11743-013-1469-x.

[16] Kruszelnicka, I., Ginter-Kramarczyk, D., Wyrwas, B., Idkowiak, J. (2019). Evaluation of surfactant removal efficiency in selected domestic wastewater treatment plants in Poland. *Journal of Environmental Health Science and Engineering*, 17(2), 1257–1264. DOI: 10.1007/s40201-019-00387-6.

[17] Wu, Z., Deng, W., Tang, S., Ruiz-Hitzky, E., Luo, J., Wang, X. (2021). Pod-inspired MXene/porous carbon microspheres with ultrahigh adsorption capacity towards crystal violet. *Chemical Engineering Journal*, 426, 130776. DOI: 10.1016/j.cej.2021.130776.

[18] Huang, Z., Li, Y., Chen, W., Shi, J., Zhang, N., Wang, X., Li, Z., Gao, L., Zhang, Y. (2017). Modified bentonite adsorption of organic pollutants of dye wastewater. *Materials Chemistry and Physics*, 202, 266–276. DOI: 10.1016/j.matchemphys.2017.09.028.

[19] Sahnoun, S., Boutahala, M., Tiar, C., Kahoul, A. (2018). Adsorption of tartrazine from an aqueous solution by octadecyltrimethylammonium bromide-modified bentonite: Kinetics and isotherm modeling. *Comptes Rendus Chimie*, 21(3–4), 391–398. DOI: 10.1016/j.crci.2018.01.008.

[20] Ranjani, G.I.S., Ramamurthy, K. (2010). Analysis of the Foam Generated Using Surfactant Sodium Lauryl Sulfate. *International Journal of Concrete Structures and Materials*, 4(1), 55–62. DOI: 10.4334/IJCSM.2010.4.1.055.

[21] Handayangi, L. (2020). Pengaruh Kandungan Deterjen Pada Limbah Rumah Tangga Terhadap Kelangsungan Hidup Udang Galah (Macrobracium Rosenbergh). *Sebatik*, 24(1), 75-80.

[22] Belladona, M. (2017). Analisis Tingkat Pencemaran Sungai Akibat Limbah Industri Karet di Kabupaten Bengkulu Tengah. In: *Prosiding Seminar Nasional Sains dan Teknologi Fakultas Teknik Universitas Muhammadiyah Jakarta 2017*. Jakarta.

[23] Yang, D., Cheng, F., Chang, L., Wu, D. (2022). Sodium Modification of Low Quality Natural Bentonite as Enhanced Lead Ion Adsorbent. *Colloids and Surfaces A: Physicochemical and Engineering Aspects*, 651, 129753. DOI: 10.1016/j.colsurfa.2022.129753.

[24] Sirait, M., Bukit, N., Siregar, N. (2017). Preparation and characterization of natural bentonite in to nanoparticles by co-precipitation method. *AIP Conference Proceedings*, 1801, 020006. DOI: 10.1063/1.4973084.

[25] Tabak, A., Afsin, B., Caglar, B., Koksal, E. (2007). Characterization and pillaring of a Turkish bentonite (Resadiye). *Journal of Colloid and Interface Science*, 313(1), 5–11. DOI: 10.1016/j.jcis.2007.02.086.

[26] Ajemba, R.O. (2014). Structural Alteration of Bentonite From Nkaliki by Acid Treatment: Studies of The Kinetics and Properties of The Modified Samples. *International Journal of Advances in Engineering & Technology*, 7(2), 379-392. DOI: 10.7323/ijaet/v7_iss2.

[27] Madejová, J.., Kečkéš, J.., Pálková, H., Komadel, P.. (2002). Identification of components in smectite/kaolinite mixtures. *Clay Minerals*, 37(2), 377–388. DOI: 10.1180/0009855023720042.

[28] Al-Essa, K., Al-Essa, E.M. (2021). Effective Approach of Activated Jordanian Bentonite by Sodium Ions for Total Phenolic Compounds Removal from Olive Mill Wastewater. *Journal of Chemistry*, 2021, 7405238. DOI: 10.1155/2021/7405238.

[29] Mekhamer, W.K. (2016). Energy storage through adsorption and desorption of water vapour in raw Saudi bentonite. *Arabian Journal of Chemistry*, 9, S264–S268. DOI: 10.1016/j.arabjc.2011.03.021.

[30] Karelius, K., Sadiana, I.M., Fatah, A.H., Agnestisia, R. (2022). Co-Precipitation Synthesis of Clay-Magnetite Nanocomposite for Adsorptive Removal of Synthetic Dye in Wastewater of Benang Bintik Batik. *Molekul*, 17(2), 261. DOI: 10.20884/1.jm.2022.17.2.6358.

[31] Batdemberel, G., Battumur, T., Enkhtuya, T., Tsermaa, G., Chadraabal, S. (2015). Synthesis of ZnO Nanoparticles by Mechanochemical Processing. In: *Proceedings of the 4th International Conference on X-ray Analysis*. Mongolia.

[32] Mu'azu, N.D., Jarrah, N., Kazeem, T.S., Zubair, M., Al-Harthi, M. (2018). Bentonite-layered double hydroxide composite for enhanced aqueous adsorption of Eriochrome Black T. *Applied Clay Science*, 161, 23–34. DOI: 10.1016/j.clay.2018.04.009.

[33] Tong, D.S., Wu, C.W., Adebajo, M.O., Jin, G.C., Yu, W.H., Ji, S.F., Zhou, C.H. (2018). Adsorption of methylene blue from aqueous solution onto porous cellulose-derived carbon/montmorillonite nanocomposites. *Applied Clay Science*, 161, 256–264. DOI: 10.1016/j.clay.2018.02.017.

[34] Hakim, Y., Mohadi, R., Mardiyanto, M., Royani, I. (2023). Ammonium-Assisted Intercalation of Java Bentonite as Effective of Cationic Dye Removal. *Journal of Ecological Engineering*, 24(2), 184–195. DOI: 10.12911/22998993/156665.

[35] Sing, K.S.W., Williams, R.T. (2005). Empirical Procedures for the Analysis of Physisorption Isotherms. *Adsorption Science & Technology*, 23(10), 839–853. DOI: 10.1260/026361705777641990.

[36] Mohadi, R., Normah, N., Fitri, E.S., Palapa, N.R. (2022). Unique Adsorption Properties of Cationic Dyes Malachite Green and Rhodamine-B on Longan (Dimocarpus longan) Peel. *Science and Technology Indonesia*, 7(1), 115–125. DOI: 10.26554/sti.2022.7.1.115-125.

[37] Messaoudi, M., Douma, M., Tijani, N., Dehmani, Y., Messaoudi, L. (2021). Adsorption process of the malachite green onto clay: kinetic and thermodynamic studies. *Desalination and Water Treatment*, 240, 191–202. DOI: 10.5004/dwt.2021.27688.

[38] Kalam, S., Abu-Khamsin, S.A., Kamal, M.S., Patil, S. (2021). Surfactant Adsorption Isotherms: A Review. *ACS Omega*, 6(48), 32342–32348. DOI: 10.1021/acsomega.1c04661.

[39] Elmorsi, T.M. (2011). Equilibrium Isotherms and Kinetic Studies of Removal of Methylene Blue Dye by Adsorption onto Miswak Leaves as a Natural Adsorbent. *Journal of Environmental Protection*, 02(06), 817–827. DOI: 10.4236/jep.2011.26093.

[40] Langmuir, I. (1916). The Constitution and Fundamental Properties of Solids and Liquids. *Journal of the American Chemical Society*, 38(11), 2221–2295. DOI: 10.1021/ja02268a002.

[41] Foo, K.Y., Hameed, B.H. (2010). Insights into the modeling of adsorption isotherm systems. *Chemical Engineering Journal*, 156(1), 2–10. DOI: 10.1016/j.cej.2009.09.013.

[42] Zhu, S., Wang, D. (2017). Photocatalysis: Basic Principles, Diverse Forms of Implementations and Emerging Scientific Opportunities. *Advanced Energy Materials*, 7(23), 1700841. DOI: 10.1002/aenm.201700841.

[43] Zhang, F., Li, S., Zhang, Q., Liu, J., Zeng, S., Liu, M., Sun, D. (2019). Adsorption of different types of surfactants on graphene oxide. *Journal of Molecular Liquids*, 276, 338–346. DOI: 10.1016/j.molliq.2018.12.009.

[44] Jabar, J.M., Odusote, Y.A., Alabi, K.A., Ahmed, I.B. (2020). Kinetics and mechanisms of congo-red dye removal from aqueous solution using activated Moringa oleifera seed coat as adsorbent. *Applied Water Science*, 10(6), 136. DOI: 10.1007/s13201-020-01221-3.

[45] Malima, N.M., Owonubi, S.J., Lugwisha, E.H., Mwakaboko, A.S. (2021). Thermodynamic, isothermal and kinetic studies of heavy metals adsorption by chemically modified Tanzanian Malangali kaolin clay. *International Journal of Environmental Science and Technology*, 18(10), 3153–3168. DOI: 10.1007/s13762-020-03078-0.

[46] Zhang, Y., Shi, W., Zhou, H., Fu, X., Chen, X. (2010). Kinetic and Thermodynamic Studies on the Adsorption of Anionic Surfactant on Quaternary Ammonium Cationic Cellulose. *Water Environment Research*, 82(6), 567–573. DOI: 10.2175/106143009X12529484816079.

[47] Zhang, P., Liu, Y., Li, Z., Kan, A.T., Tomson, M.B. (2018). Sorption and desorption characteristics of anionic surfactants to soil sediments. *Chemosphere*, 211, 1183–1192. DOI: 10.1016/j.chemosphere.2018.08.051.

[48] Li, P., Ishiguro, M. (2016). Adsorption of anionic surfactant (sodium dodecyl sulfate) on silica. *Soil Science and Plant Nutrition*, 62(3), 223–229. DOI: 10.1080/00380768.2016.1191969.

[49] Herawati, I., Permadi, P., Rochliadi, A., Marhaendrajana, T. (2022). Adsorption of anionic surfactant on sandstone reservoir containing clay minerals and its effect on wettability alteration. *Energy Reports*, 8, 11554–11568. DOI: 10.1016/j.egyr.2022.08.268.

[50] Abbas, A.H., Pourafshary, P., Wan Sulaiman, W.R., Jaafar, M.Z., Nyakuma, B.B. (2021). Toward Reducing Surfactant Adsorption on Clay Minerals by Lignin for Enhanced Oil Recovery Application. *ACS Omega*, 6(29), 18651–18662. DOI: 10.1021/acsomega.1c01342.